Journal of Molecular Liquids 386 (2023) 122503

Contents lists available at ScienceDirect

Journal of Molecular Liquids

journal homepage: www.elsevier.com/locate/molliq

Selective molecular recognition of amino acids and their derivatives by cucurbiturils in aqueous solution: An MD/3D-RISM study

Natthiti Chiangraeng [a,b], Haruyuki Nakano [c], Piyarat Nimmanpipug [a,b,*], Norio Yoshida [d,*]

[a] Department of Chemistry, Faculty of Science, Chiang Mai University, Chiang Mai 50200, Thailand
[b] Materials Science Research Center, Faculty of Science, Chiang Mai University, 239 Huay Kaew Road, Suthep, Muang, Chiang Mai, 50200, Thailand
[c] Department of Chemistry, Graduate School of Science, Kyushu University, 744 Motooka, Nishi-ku, Fukuoka 819-0395, Japan
[d] Department of Complex Systems Science, Graduate School of Informatics, Nagoya University, Chikusa-ku, Nagoya 464-8601, Japan

ARTICLE INFO

Keywords:
Molecular recognition
Cucurbituril
Amino acid
Solvation
3D-RISM

ABSTRACT

The three-dimensional reference interaction site model theory was utilized to investigate cucurbituril–guest binding and its corresponding solvation structure. In this study, glycine, tryptophan, phenylalanine and their derivatives were employed as representatives of guest molecules. In the case of aromatic amino acids, phenylalanine shows the most significant binding affinity in cucurbit-7-uril, whereas tryptophan provides the highest binding affinity in cucurbit-8-uril. Although these guest molecules are very similar in molecular volumes, their chemical and physical properties are different. These findings agree well with reports from previous studies. We also found that the substitution of the *tert*-butyl ($-C(CH_3)_3$) group at the *para*-position in phenylalanine provides the highest binding affinity gain among all derivatives. Moreover, the unbound state of glycine is pointed out.

1. Introduction

The study of molecular recognition of amino acids via supramolecular host–guest chemistry is an essential and challenging task for molecular sensing of biomolecules and in disease diagnostic fields [1]. Molecular recognition is regarded as one of the fundamental processes in biological systems, in which a guest molecule binds to a host with specific nonbonded interactions and relatively high affinity [2,3]. Investigation via a theoretical viewpoint is a promising tool for offering deeply insightful perceptions into host–guest interactions and the effects of crucial phenomena on binding affinity gains. Not only general ideas can be perceived in this study, but these findings will also contribute to scientific viewpoints when designing host–guest systems for sophisticated and specific applications [1–3].

Cucurbit[*n*]uril CB*n* is a member of the macrocycle family synthesized via a condensation reaction of glycoluril with formaldehyde, forming macrocyclic molecules containing *n* glycoluril units (see Fig. 1) [2,4,5]. It has identical carbonyl groups around portals with relatively high polarity and polarizability. At the same time, its inner cavity is hydrophobic, preferably leading to encapsulating neutral or positive guest molecules [2,4–6] via noncovalent interactions such as electrostatic interactions and hydrogen bonding. The carbonyl groups around the portals can form hydrogen bonding with the solvent water and guest, which contributes to the binding affinity gain and stability between host and guest molecules [7]. The factor involving the binding affinity of amino acids and their derivatives in an aqueous solution can be unclear because functional groups in the amino acid structure can form hydrogen bonding between the solvent water and CB host [8,9]. With tunable sizes in CBs, they provide different binding affinities when binding with a guest molecule according to the physical and chemical properties of the molecule [2,4–6]. Therefore, to design a complex with high affinity and selectivity, we need to exploit these properties between host and guest molecules properly and carefully.

The dominant feature of CBs is their significant selectivity to physical and chemical properties of guest molecules when forming complex structures, i.e., size, shape, hydrophobic/hydrophilic contribution, functional group, binding structure and so on [2,4,6]. These factors are crucial to investigate the host–guest complexation and its related binding energy. Many studies of a variety of guest molecules binding to CBs of different sizes have been reported [1,2,5]. Among these reports, CBs with *n* of 6–8 are mostly examined in terms of experimental and computational viewpoints because of their water solubility and low toxicity. Accordingly, CB–guest binding systems have attracted much interest in various fields, including antiviral [10], drug carrier [5,11–14]

* Corresponding authors at: Department of Chemistry, Faculty of Science, Chiang Mai University, Chiang Mai 50200, Thailand (P. Nimmanpipug), Department of Complex Systems Science, Graduate School of Informatics, Nagoya University, Nagoya 464-8601, Japan (N. Yoshida).
E-mail addresses: piyarat.n@cmu.ac.th (P. Nimmanpipug), noriwo@nagoya-u.jp (N. Yoshida).

https://doi.org/10.1016/j.molliq.2023.122503
Received 15 May 2023; Received in revised form 26 June 2023; Accepted 2 July 2023
Available online 4 July 2023

and sensor [5,15–17]. However, investigations of amino acids as guest molecules have been seldom explored and revealed in detail.

Amino acids are a fundamental unit of peptides and proteins consisting of 20 different molecular structures. Examining amino acids bound with CBs as a host–guest system can provide insightful information on selectivity in terms of binding affinity, leading to the design of a molecular sensor for diagnostic applications [5,18,19]. Zheng and coworkers reported that amino acids can provide inclusion, partial inclusion and exclusion complexes with CB7 using traditional molecular dynamics simulations [20]. Molecules with relatively small side chains, including glycine, alanine, serine and aspartic acid, lead to exclusion complexes, whereas the rest form inclusion or partial inclusion complexes. In the case of CB6, Shan et al. shown that glycine can provide both inclusion and exclusion complexes, depending on the relative amounts of CB6 and glycine [21]. The mole equality between host and guest molecules leads to the inclusion complex for this case. According to previous reports, aromatic amino acids such as phenylalanine provide a greater binding affinity for CBs due to stabilized interactions from ion–dipole and van der Waals interactions [1,16,22].

Many researchers have attempted to investigate and clarify the role of various factors in the complexation process of CBs and amino acids [1,16,22]. However, these findings lack universality and do not apply to all cases due to differences in the intrinsic properties of the guest molecule. The solid evidence to support a greater understanding of high binding affinity gain in this system is the release of water molecules in the CB cavity, known as "*high-energy water*" [23–25]. The "*high-energy water*" was regarded in terms of the required energy for breaking hydrogen bonds between water molecules inside the CB cavity and the CB structure in host–guest complexation processes [6,24]. Such water molecules have a higher intermolecular interaction energy compared with the water molecules in bulk and have higher solvation free energy (SFE). To investigate this phenomenon of changing solvent water, an appropriate calculation method should be selected to handle this problem.

To investigate the complexation process of amino acids with CBs in detail as well as the influences of surrounding environments in the aqueous solution, the three-dimensional reference interaction site model (3D-RISM) theory was chosen to achieve our goal. The 3D-RISM theory is based on statistical mechanics derived from the molecular Ornstein–Zernike equation [3,26,27]. This theory can properly handle solvation properties based on an explicit intermolecular interaction to represent the properties and phenomena of a molecular recognition system in an aqueous solution [3,6]. The 3D-RISM can calculate the partial molar volume (PMV) change ($\Delta\overline{V}$) and the SFE of the system from the reorganization of solvent water, which is crucial for the investigation of solute and solvent interactions [28–30]. Recently, we used 3D-RISM calculations to show the molecular recognition of small organic molecules with CBs of different sizes [6]. We found that the binding affinity gains are in line with the results from the available experimental reports and conventional Molecular Mechanics/Poisson–Boltzmann Surface Area (MM/PBSA). Not only the contributions of direct interaction between the host and guest molecules are obtained from the calculation, but corresponding solvation structures due to complexation can be determined.

According to literature reviews, understanding the nature of interactions between host cucurbiturils and amino acid-based guests would contribute to a fascinating concept to improve the sensitivity and selectivity of molecular sensors for some amino acids, peptides, proteins or diseases of interest. To the best of our knowledge, there is no systematic study on the nature of interactions contributing from amino acid guests and their derivatives with cucurbituril hosts of different sizes. Therefore, CB6, CB7 and CB8 were selected as supramolecular hosts due to their reported relatively high solubility parameters in water. Phenylalanine and its derivatives were chosen as representative guests because the formal studies provided high binding affinity [1,16,19,31,32]. Glycine, the smallest amino acid, and tryptophan, which has a molecular volume close to that of phenylalanine, were employed for comparison. Representations of the chemical structures for all guest molecules are shown in Fig. 2. In this study, 3D-RISM calculations were used to study CB–guest binding in an aqueous solution. An understanding of the complexation in CBs with amino acids has provided solid evidence of their feasible applications to fields of biological interest [5].

2. Computational details

2.1. Preparation of structures and partial charge evaluation

All initial structures of guest molecules were created using the structural amino acid templates available in the GaussView 6.0 program [33]. According to previous studies, the amino acids and their derivatives are in the zwitterionic form (see Fig. 2) [34–36]. The initial structures of host and guest molecules were first optimized using density functional theory (DFT) implemented in Gaussian 16 [37]. All molecules were optimized with a calculation level of B3LYP/6-31G in an aqueous solution without any symmetry constraints. The conductor-like polarizable continuum model (CPCM) was used to include the effect of implicit solvent water in this study [38,39].

2.2. Molecular dynamics (MD) simulations

Before performing an MD simulation, the Antechamber tool [40] was used to prepare the potential parameters based on the general Amber force field (GAFF) and assign partial charges from the Gaussian output

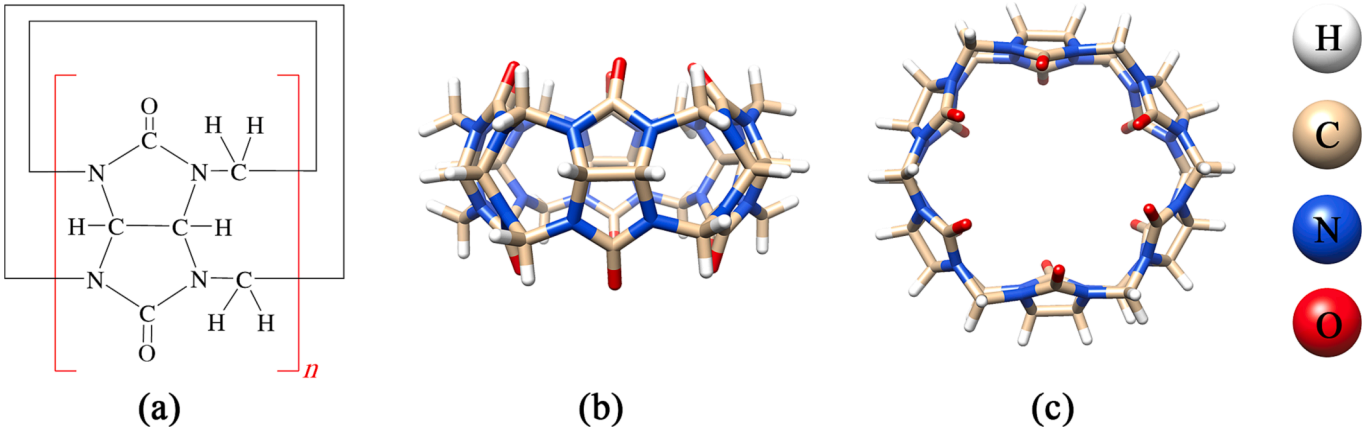

Fig. 1. (a) Chemical structures of cucurbituril, where *n* is the number of glycoluril units, 6–8. (b) and (c) depict the side and top views of CB6 as examples.

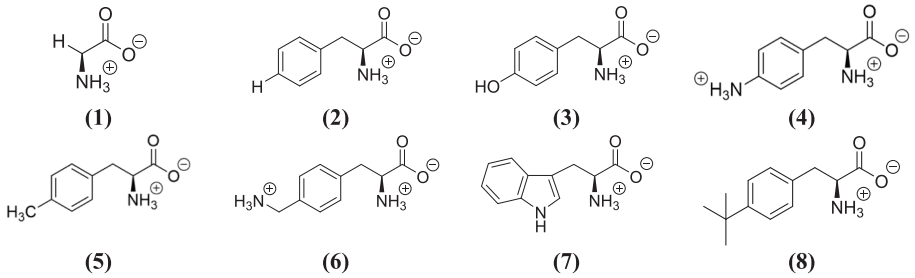

Fig. 2. Chemical structures of guest molecules and corresponding abbreviations used in this work.

files to the molecules. The effective point charges based on the restrained electrostatic potential (RESP) charge method were also calculated using DFT calculations. To represent a host–guest complex in the real environment, we used the TIP3P [41] solvent water model for explicit water simulations. With this model, 1300–3000 water molecules were added to hydrate CBs, guests, and their complexes, resulting in an approximate simulation box size between 60,000 and 120,000 $Å^3$. All topology and coordinate files for MD calculations were generated using the tleap module implemented in the Amber program [42].

In this study, MD simulations were carried out using Amber20 software [42]. All systems were performed in the same conditions. First, the PMEMD.MPI was utilized in an energy minimization step to prepare a suitable structure for an MD simulation. A combination of the steepest descent and conjugate gradient methods was utilized subsequently, with a cycle of 5000 steps in each technique. After that, the isothermal–isobaric ensemble was performed for 2 μs. The Berendsen thermostat and barostat were used to control temperature and pressure, respectively [43]. The temperature and pressure of 300 K and 1 atm, respectively, were used. The SHAKE algorithm was also applied in this study [44].

2.3. Analysis of internal interaction energy components and system properties

In MD simulations, the CPPTRAJ module [45] was utilized to calculate the internal interaction energies from each structure sample. This module can also be used to calculate the root-mean-square deviation (RMSD). The RMSD results can be first used to confirm an equilibrium in each system. In this study, the RMSD profiles indicate that all systems reached the equilibrium in a simulation time of approximately 1 μs (see Figs. S1, S2). The results show that the CB8–**1** complex attained a stable complex structure after 0.6 μs. Therefore, 1000 sampled structures from the rest of the 1 μs were used for further analysis and subsequently utilized as input structures for 3D-RISM calculations for all systems.

2.4. 3D-RISM calculations

Both CBs and hosts were treated as solute molecules, whereas water molecules were treated as a solvent in a 3D-RISM calculation. With this 3D-RISM calculation, the solute molecules are assumed to be in finite dilution. Before performing a 3D-RISM analysis, the structure samples from an MD simulation need to be manipulated. We stripped the explicit water molecules from all structure samples; then, the water was regenerated by the 3D-RISM method. The KH closure [27,46] was selected because of the proven rapid convergence from formal studies [47]. The same force field parameters with the MD simulation were employed for the 3D-RISM calculation. The number of grid points of 128^3 was utilized in this study with a grid spacing of 0.5 Å. The 3D-RISM calculations were performed using our in-house codes implemented with the reference interaction site model integrated calculator (RISMiCal) package [48–50]. In the case of a 3D-RISM calculation, no further postprocessing is required. All thermodynamic and system properties were printed out in the output files for each selected structure sample.

3. Results and discussion

3.1. Host–guest binding features

Before conducting an energy component analysis, a host–guest binding feature should be considered to ensure consistent binding structures for the subsequent energy component analysis. From MD trajectories, we found that almost all complexes have an inclusion binding feature; a guest binds inside the CB cavity as depicted in Fig. 3, whereas different features show exclusion complexes; a guest binding from the outside of the CB cavity (see Fig. 3) has been observed in the CB7–**1** and CB8–**1** complexes. From our results, the inclusion binding feature of the CB6–**1** complex is in line with the experimental findings of aqueous solution and solid–state samples [21]. Shan and coworkers reported that a binding feature of the CB6–**1** complex could be an inclusion or exclusion complex, depending on the amount of CB and guest molecules in the solution [21]. In the case of the CB7–**1** exclusion complex, Ma et al. computationally shown that the side chain of guest **1** is too small and has a tiny binding entropy gain, leading to a difficult encapsulation into the sizeable hydrophobic cavity of CB7 [20]. This finding also agrees well with our results.

The rest of the guest molecules provide inclusion complexes for all CBs. Guests **3**, **6** and **7** show bridge hydrogen bonding (HB) interactions at the two CB portals, whereas guests **1**, **2**, **4**, **5** and **8** form a one-way HB interaction with only one portal due to containing the hydrophobic part at the end of the substituent group as depicted in Fig. 3 and Fig S3. According to binding structures, the protonated amine groups of guest molecules are preferentially positioned to form an HB interaction with the carbonyl groups of the CB portal. Another end of a hydroxyl group also forms HB. This finding is consistent with the study by Bodoor and coworkers [7]. They reported that nitrogen atoms of guest molecules are closely positioned around a CB portal and form HB with the carbonyl groups of the CB portal [7]. It should be noted that we found an unbound state in the cases of CB7–**1** and CB8–**1** complexes. In this unbound state, guest **1** and CB structures completely locate far away from each other.

To provide insightful information about the binding and unbound states in the CB7–**1** and CB8–**1** complexes, we collected sampling snapshots of up to 2000 structures to obtain a sufficient number of snapshots for each state, which is more than our ordinary method provided above. In this investigation, these structures were also obtained from the last 1 μs in the production stage of an MD simulation. According to a trajectory analysis, several binding and unbound states were differentiated and are shown in Fig. 4. This figure clearly shows that the higher complex energy is in the unbound state compared with that of the binding state for both complexes. The number of binding state structures is higher than that of unbound state structures. These results partly indicate that each complex's structure in the binding state shows superior stability. However, we cannot make a concrete conclusion about the stability until we investigate the energy component analysis in these systems. To this end, the structures from both states will be considered in further analyses separately, binding and unbound complex structures.

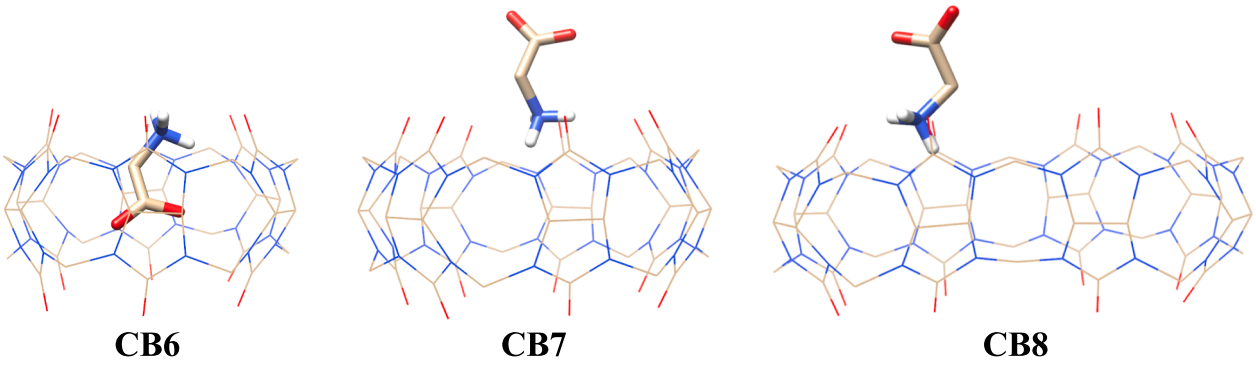

Fig. 3. Snapshots of binding states for CB*n*–**1** complexes.

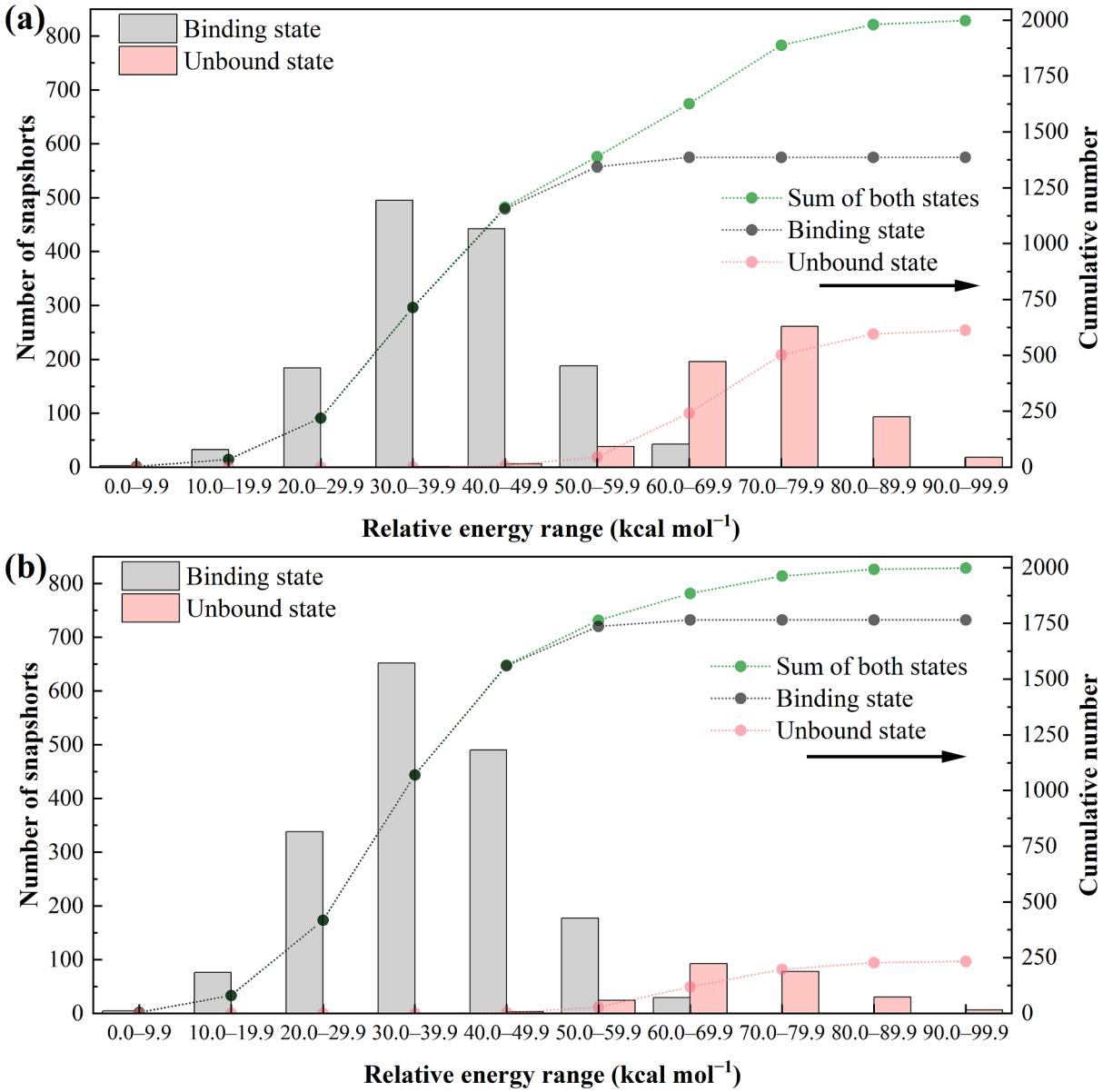

Fig. 4. Number of snapshots in each energy range and its cumulative number: (a) CB7–**1** and (b) CB8–**1** complexes. These 2000 snapshots were sampled from the last 1 μs of MD simulations. The axis of abscissa is depicted as the relative energy of a complex.

The obtained results will be later explained in detail.

3.2. Individual properties of free CBs and guests

For a CB–guest complex system, various factors mutually influence the binding affinity gain [6,11,20,24,25,51–54], and molecular size is a typical factor to be considered. We can assess the size fit between a guest and a CB cavity using the molecular size [6]. Guests with similar molecular size and chemical and physical properties are likely to have a similar magnitude of binding affinity, *e.g.*, a guest and its derivatives.

In this study, the molecular volume represented by $\Delta\overline{V}$ can be obtained from 3D-RISM calculation, which is expressed as follows [55]:

$$\Delta\overline{V} = k_B T \chi_T \left[1 - \rho \sum_{\gamma \in \text{solvent}} c_\gamma(\boldsymbol{r}) \mathrm{d}\boldsymbol{r} \right]. \quad (1)$$

χ_T is the isothermal compressibility of the solution obtained from the site–site correlation function. c_γ is the direct correlation function of solvent site γ obtained by the 3D-RISM calculation. k_B, T, and ρ denote the Boltzmann constant, absolute temperature and number density of solvent water, respectively. This $\Delta\overline{V}$ is calculated using the Kirkwood–Buff equation generalized to the interaction site representation of liquid and solutions and well represents the size of a molecule in solution.

The solvation property is a primary property to be considered before investigating the binding affinity and its components in detail. This property is contributed by interaction energy obtained from a conventional MD simulation and SFE obtained from a 3D-RISM calculation [6]. The formalisms relevant to our discussion will be described throughout this work, and further detailed information can be found in formal studies [3,27,29,56,57].

The total free energy G of an individual system is defined as

$$G = E_{\text{mm}} + G_{\text{solv}}, \quad (2)$$

where E_{mm} and G_{solv} are the solute internal potential energy and SFE, respectively.

Fig. 5 shows the molecular volume and SFE of individual CB and guest molecules. The CB-size dependence of SFE can be observed in the case of CB structures. In contrast, the SFEs of guest molecules are independent of molecular guest sizes. In Fig. 5d, guests **4** and **6** provide highly negative values of SFE due to their positively charged guests. Despite guest **1** having the smallest size in this study, its SFE value is very similar to those of the other neutral guests (guests **2**, **3**, **5**, **7** and **8**). Note that guest **7** has different chemical and physical properties from the others because it contains a nonaromatic residue (indole ring) but also provides consistent SFE values.

3.3. Energy component analysis and corresponding solvation structures

The energy component analysis utilizing combined results from MD simulations and 3D-RISM calculations can provide insight into contributions that influence a binding affinity gain. According to equation (2), the binding free energy ΔG_{bind} of a complex system can be given by

$$\Delta G_{\text{bind}} = \Delta E_{\text{mm}} + \Delta G_{\text{solv}}. \quad (3)$$

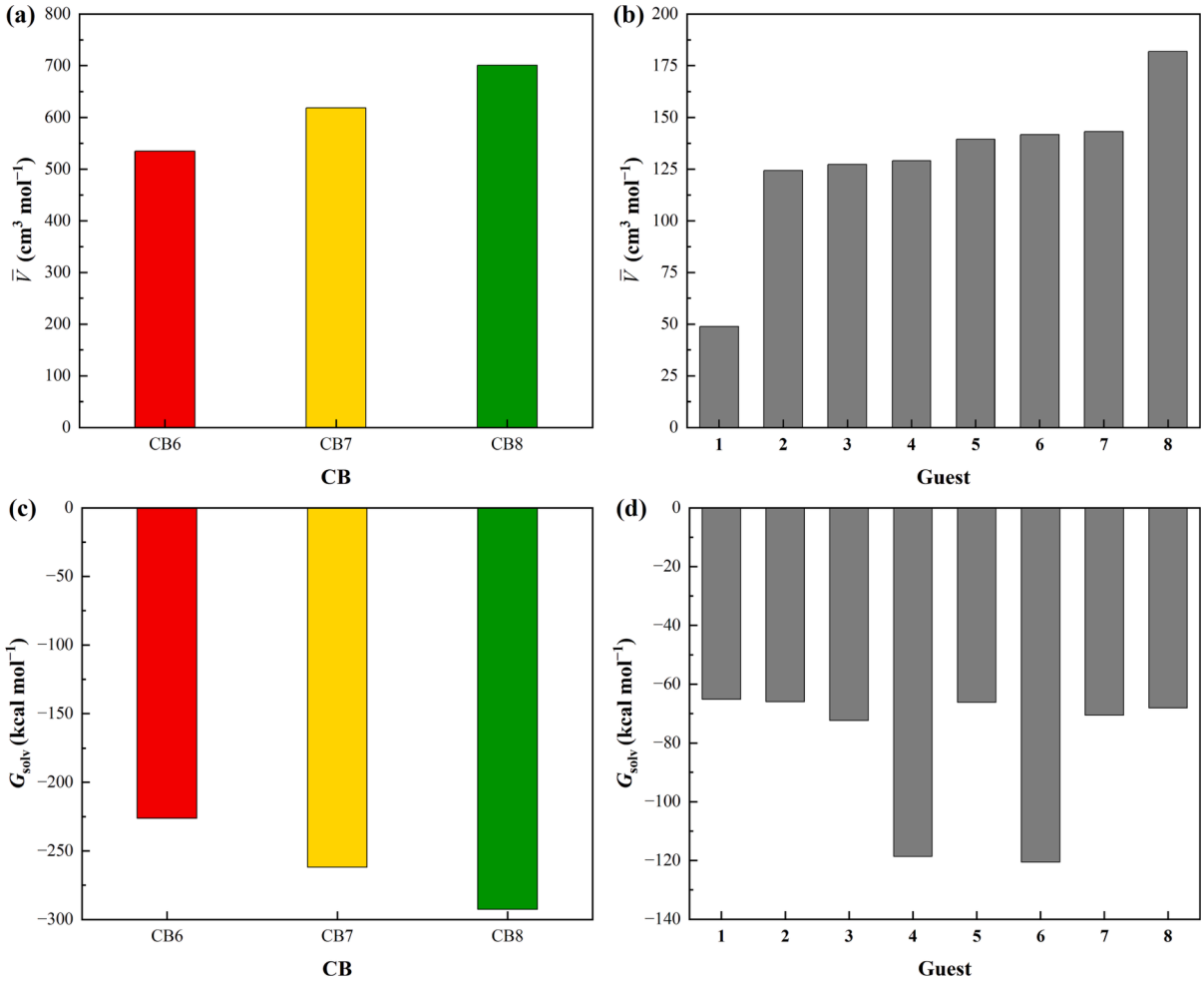

Fig. 5. $\overline{V}$ and solvation free energy (G_{solv}) of (a, c) CBs and (b, d) guests, respectively.

The internal energy change ΔE_{mm} is analyzed from MD trajectories, which can be expressed as

$$\Delta E_{mm} = E_{complex} - \left(E_{CB} + E_{guest}\right), \quad (4)$$

where E_{CB}, E_{guest}, and $E_{complex}$ are the internal energies with respect to CB*n*, guest and the CB*n*–guest complex, respectively. In the calculation, the change in SFE ΔG_{solv} can be written as

$$\Delta G_{solv} = G_{solv}^{complex} - \left(G_{solv}^{CB} + G_{solv}^{guest}\right), \quad (5)$$

where G_{solv}^{CB}, G_{solv}^{guest}, and $G_{solv}^{complex}$ are the SFEs with respect to CB*n*, guest and the CB*n*–guest complex, respectively.

Fig. 6 shows the binding free energy and its components for all complexes. Apart from the unbound systems, the ΔE_{mm} has negative values, whereas ΔG_{solv} is positive. The unbound systems show inverse trends to this line and provide positive values for the binding affinity gain. We found that CB6–**1** and CB6–**7** also deliver positive binding affinities, indicating an unfavorable host–guest binding. This finding agrees with the previous experimental report from Buschmann and coworkers [36]. They reported that the thermal effect of the CB6–**1** complex is too small for the calculation of stability constants. In the case of binding complexes, two apparent trends of the ΔG_{bind} can be noticed: (I) aimed at guests **1** and **7,** CB8–guest complexes show superior binding free energies, and (II) for guest **2** and its derivatives (guests **3**, **4**, **5**, **6** and **8**), CB7–guest complexes show greater binding affinity gains. According to these behaviors, further results and discussion will be made based on these manners of binding. The unbound states in the CB7–**1** and CB8–**1** complexes will be described separately from other host–guest systems.

The contributions of components of ΔE_{mm} and ΔG_{solv} were further analyzed to give insightful information on energy components dominating CB–guest binding affinity. The ΔE_{mm} is composed of three components regarding the CB–guest interaction energy $\Delta E_{mm}^{interaction}$, and structural energy changes because of the binding between CB and guest molecules that are denoted as ΔE_{mm}^{guest} and ΔE_{mm}^{CB}, respectively, as follows.

$$\Delta E_{mm} = \Delta E_{mm}^{interaction} + \Delta E_{mm}^{guest} + \Delta E_{mm}^{CB}. \quad (6)$$

These components of ΔE_{mm} are depicted in Fig. 7.

The ΔG_{solv} consists of four components [58]: solute–solvent interaction energy $\Delta E_{interaction}^{uv}$, solvent reorganization energy ΔE_{reorg}^{vv}, solvation entropy change $-T\Delta\Delta S$ and an energy correction term $\Delta E_{correction}$ based on the pressure correction method [59,60], which is expressed as

$$\Delta G_{solv} = \Delta E_{interaction}^{uv} + \Delta E_{reorg}^{vv} - T\Delta\Delta S + \Delta E_{correction}. \quad (7)$$

Here, $\Delta E_{correction}$ term is evaluated by

$$\Delta E_{correction} = -P\left(\Delta V^{complex} - \Delta V^{guest} - \Delta V^{CB}\right) \quad (8)$$

where P and ΔV denote the pressure of the system and the PMV, respectively. The P and ΔV were obtained through the correlation functions evaluated by the RISM or 3D-RISM theory. These components of ΔG_{solv} are depicted in Fig. 8.

3.3.1. *Unbound structures in CB–**1** complexes*

According to previous studies, the size fit between CB and guests is a simple and noticeable factor, contributing to a binding affinity gain due to the complete dehydration of high-energy water from the cavity and/or possibly incorporating favorable interaction energy between the CB and guest molecules [6,24,25,51]. Therefore, the complexes from the smallest guest (guest **1**) in this study will be first explained.

From the MD simulations, there are two states found in the guest **1** complexes: binding and unbound states. We found that the CB7–**1** and CB8–**1** complexes provide the unbound state, whereas CB6–**1** formed

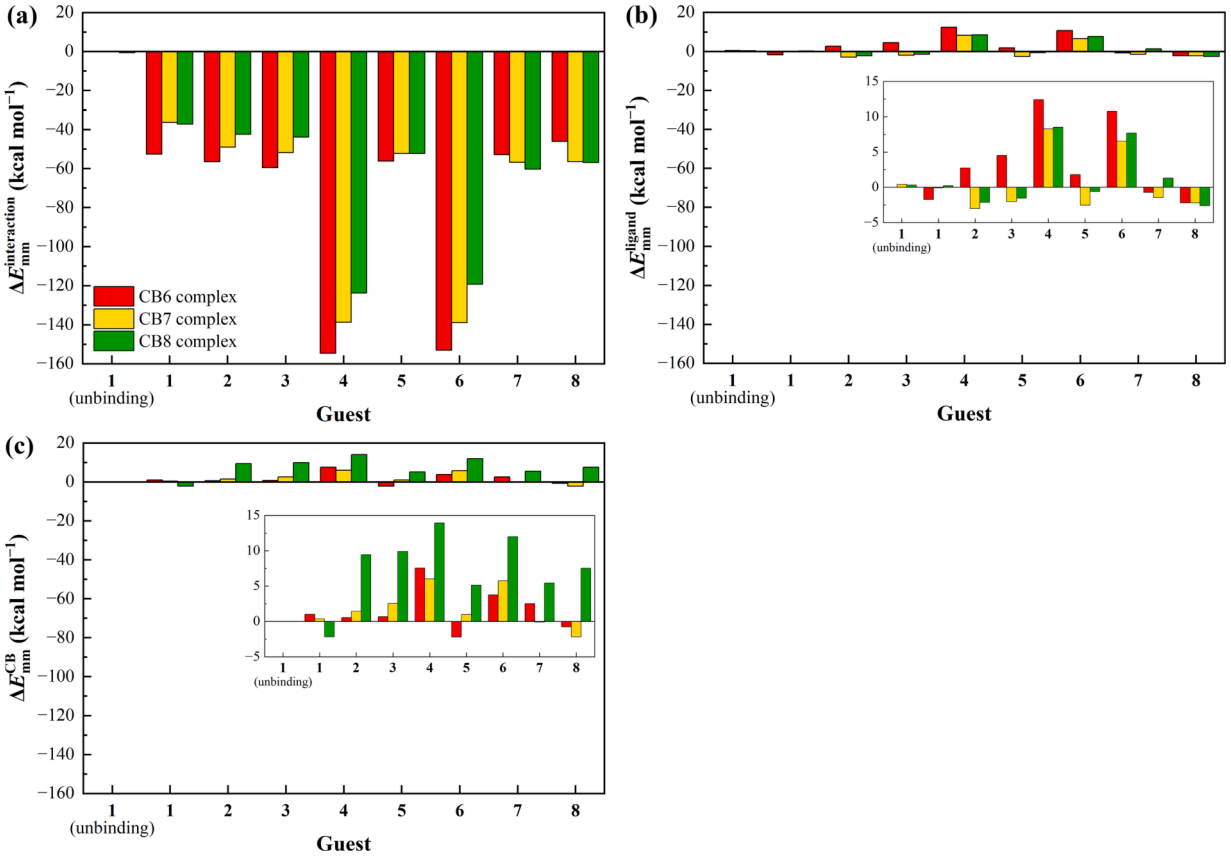

Fig. 6. Binding free energy and its components: (a) binding free energy ΔG_{bind}, (b) internal interaction energy change ΔE_{mm} and (c) solvation free energy change ΔG_{solv}.

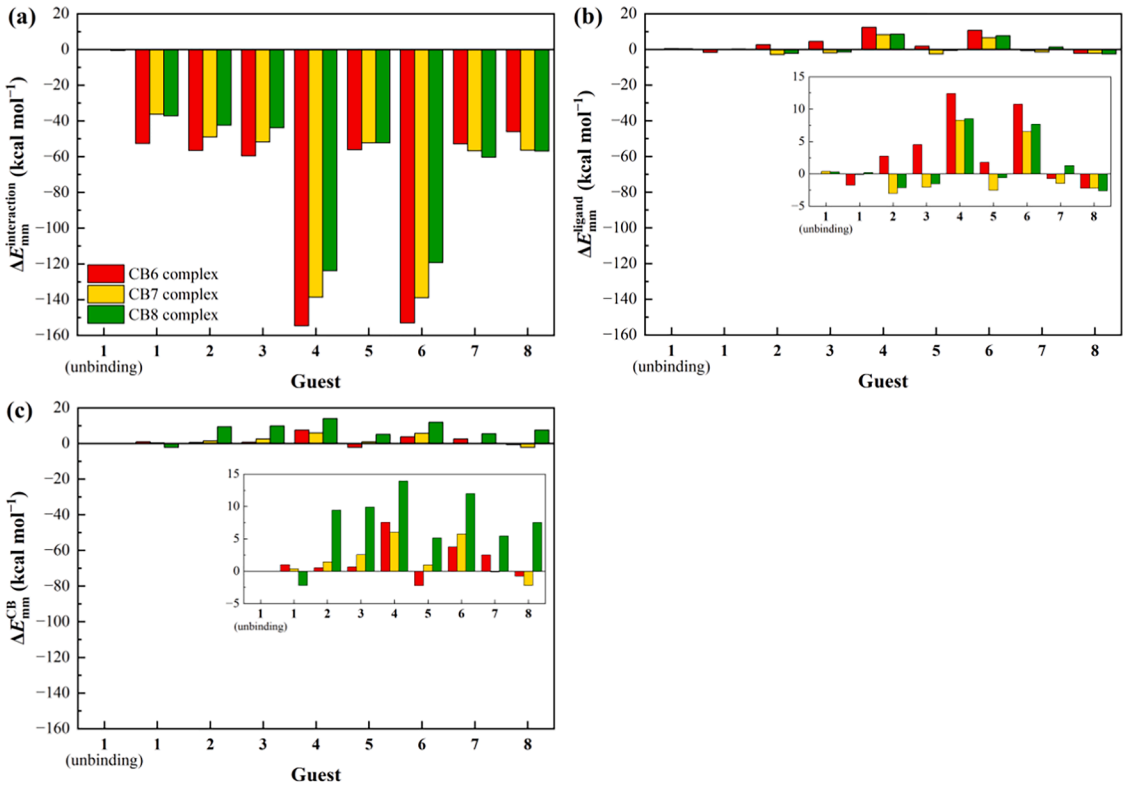

Fig. 7. Components of ΔE_{mm}: (a) CB–guest interaction energy $\Delta E_{mm}^{interaction}$ and structural energy changes because of the binding between CB and guest molecules in (b) guests ΔE_{mm}^{guest} and (c) CBs ΔE_{mm}^{CB}. The insets show a zoom-in for values close to zero.

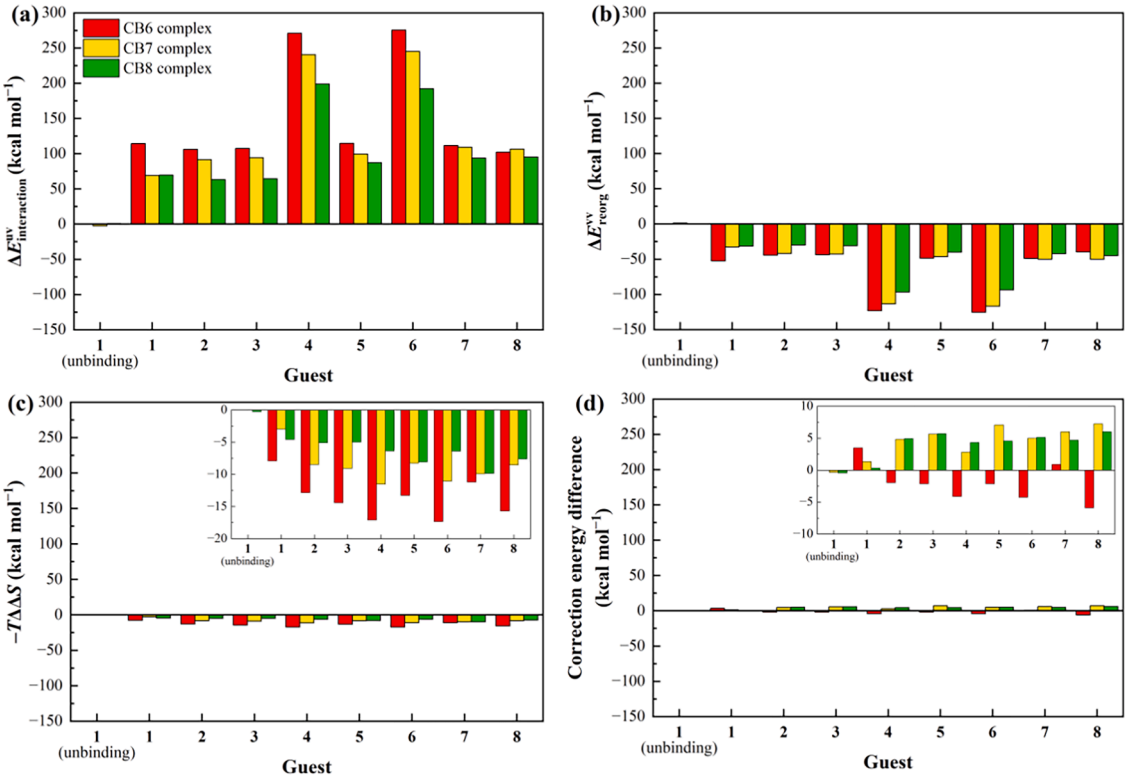

Fig. 8. Components of ΔG_{solv}: (a) solute–solvent interaction energy $\Delta E_{interaction}^{uv}$, (b) solvent reorganization energy ΔE_{reorg}^{vv}, (c) solvation entropy change $-T\Delta\Delta S$ and (d) energy correction term $\Delta E_{correction}$. The insets show a zoom-in for values close to zero.

only the binding state. In the case of the unbound state, both complexes provide positive values for ΔG_{bind}, indicating unfavorable interaction in aqueous solution as depicted in Fig. 6a. From the energy component analysis, the contribution to these positive values in ΔG_{bind} came from ΔE_{mm}, whereas ΔG_{solv} had no significant impact on ΔG_{bind}. We found that a change in the internal interaction of CB due to forming a complex, ΔE_{mm}^{CB}, plays a dominant role in this behavior. The simultaneous presence of CB and guest **1** molecules might cause ΔE_{mm}^{CB} gain. The corresponding solvation structures are depicted in Fig. 9. The figure shows that the solvation structures around the CB7 and CB8 structures from both complexes were very similar to their free structures in water (see Fig. S4). The solvent molecules distribute in the cavity and around the CB structures. This is the reason why there is no contribution from ΔG_{solv} to ΔG_{bind}.

3.3.2. *Binding structures in CB–1 and CB–7 complexes*

Apart from the unbound state, the binding states in the CB–**1** and CB–**7** complexes show the same CB-size dependence tendency for ΔG_{bind}. These complexes gained the greatest binding free energy in the case of CB8 and also shown a positive value in CB6. It is worth noting that although the same trend can be seen for these complexes, the intrinsic properties, those binding structures and solvation structures of both guest molecules are obviously different.

In the case of the CB6 complex, guest **1** shows an inclusion complex with C-terminal included inside the CB cavity. By contrast, the C-terminal of guest **7** is located outside of the CB6 cavity, and its substituent group is inside the cavity (see Fig. 10). These findings are in line with the experimental observation in the case of the CB6–**1** complex [21]. Shan and coworkers reported that the CB6–**1** inclusion complex could be achieved, depending on mole equality between CB6 and guest **1** molecules. The solvation structures demonstrate that HB can be formed between CB–guest, CB–water and guest–water molecules. This phenomenon is well-observed in the molecular recognition system in aqueous solution, and HB networks also play a crucial role in this field as pointed out in various studies [20,51,61–63]. The carbonyl groups around the CB portal form HB with the H atoms of water molecules, whereas atoms from the C-terminal and N-terminal of the amino acid also form HB with H and O of the water, respectively. At the same time, the carbonyl groups can form HB with the N-terminal of the amino acid. However, CB6–**1** and CB6–**7** complexes illustrated a similar magnitude in ΔG_{bind} with a positive quantity, indicating unfavored binding in this study.

By contrast, CB7–**1** and CB8–**1** show exclusion complexes with the C-terminal located outside the CB cavity as shown in Fig. 10. The binding feature of guest **7** complexes is similar to that of CB6–**1** complex, forming an inclusion complex for all CB sizes.

CB7–**1** and CB8–**1** exclusion complexes require relatively low dehydration penalty energy to form a complex structure compared with the CB6–**1** inclusion complex. Even though guest **1** can gain hydrophobic–hydrophobic interactions between itself and the CB cavity, resulting in lower $\Delta E_{mm}^{interaction}$ compared with larger CB sizes, the ΔG_{solv} still plays a dominant role in forming this complex, and a positive ΔG_{bind} was attained in the CB6–**1** complex. This result suggests that forming the inclusion complex between CB6 host and guest **1** molecules in water is unfavorable due to requiring high energy to dehydrate water molecules from the CB6 cavity. The small hydrophobic part in the guest **1** molecule cannot stabilize a complex structure effectively. This finding is consistent with the experimental study by Buschmann and coworkers [36]. They found that the binding affinity of the CB6–**1** complex in water solution cannot be measured because of a small heat effect in calculating stability constants and reaction enthalpies. Energy component analysis suggests that forming this CB6–**1** complex requires relatively high energy to displace water molecules compared with bigger CB cavities.

In the cases of CB7 and CB8 complexes, CB7–**1** and CB8–**1** provide negative ΔG_{bind} values because the exclusion binding does not need to displace several water molecules inside a CB cavity, resulting in a lower $\Delta E_{interaction}^{uv}$ energy requirement. From Fig. 8a, partial dehydration is required to form these complexes, so the dehydration penalty energy is reduced by half compared with forming the CB6–**1** complex. Among these complexes, CB8–**1** shows greater binding affinity due to lower $\Delta E_{mm}^{interaction}$ and ΔE_{mm}^{CB} energies as depicted in Fig. 7(a, c). This finding can be clearly explained using the snapshots depicted in Fig. S5, showing the elliptical structure of CB8 that can gain more interaction between CB8 and guest **1** molecules, and a conformation change in CB8 after complexation also contributes to greater stability in this complex.

For the case of CB–**7** complexes, we can describe them in a similar way to the CB–**1** complex, and internal interaction energy also plays a crucial role in binding affinity gain in these complexes (see Fig. 7a). The guest **7** complexes provide a superior binding affinity gain compared with guest **1** complexes, especially in the cases of CB7 and CB8, due to a major contribution of $\Delta E_{mm}^{interaction}$ in the ΔE_{mm}, indicating favorable interactions between CBs and guest **7**. In another way, the large molecular size of guest **7** also gains a more repulsive interaction with the smaller size of CBs due to cavity size limitation, corresponding to higher $\Delta E_{mm}^{interaction}$. This fact leads to the unfavorable inclusion binding in the CB6–**7** complex. Fig. S6 shows that circular and elliptical forms can be found in the CB7–**7** and CB8–**7** complexes. As mentioned, the elliptical form can stabilize a complex structure and increase interaction between CB host and guest molecules, leading to a lower value of $\Delta E_{mm}^{interaction}$. The superior binding affinity in the CB8–**7** complex came from the bridge HB in both circular and elliptical forms (Fig. S7). The CB7–**7** complex provides both bridge and one-way HBs, whereas CB6–**7** forms only a one-

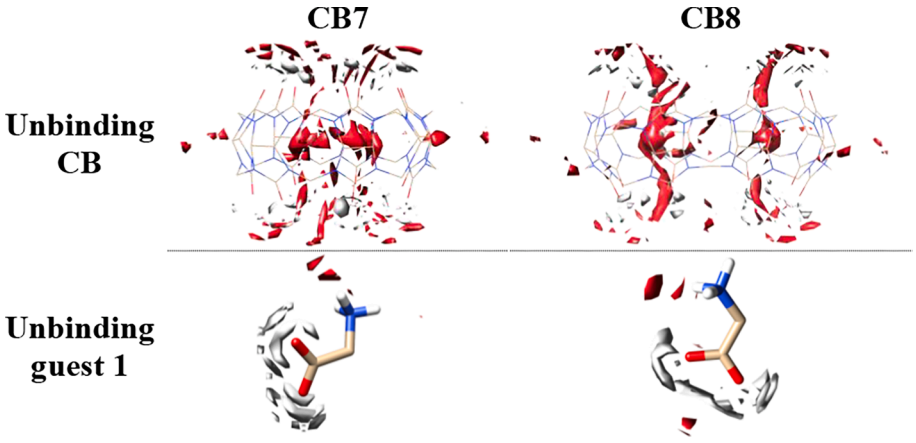

Fig. 9. Solvation structures of hosts and guest **1** in the unbound state. Isosurface plots of three-dimensional distribution functions (3D-DFs) of the water oxygen and hydrogen with $g(\boldsymbol{r}) = 4.0$ are depicted in red and white, respectively.

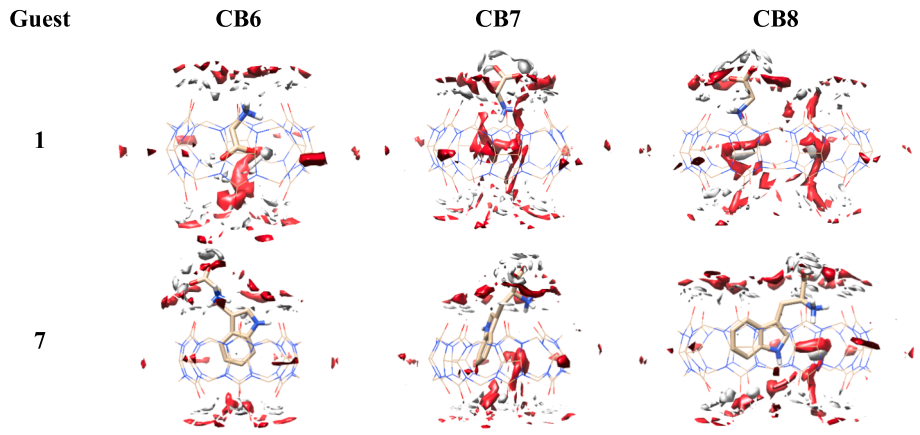

Fig. 10. Solvation structures of CB–**1** and CB–**7** complexes provide the greatest binding affinity gain in the CB8 complex. Isosurfaces of the 3D-DFs of the water oxygen and hydrogen with $g(\boldsymbol{r}) = 4.0$ are depicted in red and white, respectively.

way HB, providing the highest $\Delta E_{mm}^{interaction}$ among all CB sizes.

The requirement of a higher dehydration penalty energy for forming the CB6–**7** complex is relatively demanding; this result can also be used to support why the CB6–**7** complex provides a positive ΔG_{bind}. For the CB7–**7** and CB8–**7** complexes, the complexation also requires higher dehydration penalty energy due to its large molecular size, but it is relatively lower than the requirement for CB6–**7** complexation. Moreover, the size fit between CB hosts and guest **7** (Fig. 10 and Figs. S6, S7) plays a dominant role in the stabilization of these complexes via hydrophobic–hydrophobic interactions and HB, leading to the relatively low values of $\Delta E_{mm}^{interaction}$ in CB7–**7** and CB8–**7** complexes as plotted in Fig. 7a, resulting in lower values for ΔG_{bind}.

According to ΔG_{bind}, we found that guest **7** complexes show more stable host–guest binding than guest **1** complexes because of superior stabilization energy between CBs and guest molecules. This finding also agrees well with the previously reported results [20,31].

3.3.3. *Binding structures of guest **2** and its derivatives to CBs*

In this part, we have systematically studied the influence of substitution groups at the *para*-position (see Fig. 2) on the binding affinity gain. Guest 2 contains a H atom at the *para*-position, and it was used as a reference structure in the discussion below. Other substituents were defined as their derivatives. The substituted groups of guests **2**, **3**, **4**, **5**, **6** and **8** are hydrogen (–H), hydroxyl (–OH), ammonium ($-NH_3^+$), methyl ($-CH_3$), methylammonium ($-CH_2NH_3^+$) and *tert*-butyl ($-C(CH_3)_3$) groups, respectively, sorted by smaller to bigger molecular volumes as depicted in Fig. 5.

According to ΔG_{bind} in Fig. 6, the CB7–**2**, **3**, **4**, **5** and **6** complexes provide similar magnitude in binding affinity gain, whereas the CB7–**8** complex shows an obviously greater value. Apart from guest **8**, the substituent groups are similar in molecular volume but have distinct chemical properties and/or net charges. Overall, the ΔG_{bind} of CB7 complexes gives the highest negative values, whereas the CB6 complexes shown the highest positive values. CB8 complexes provide the medium in ΔG_{bind} between that of CB6 and CB7 complexes for all cases. This is because the CB8 cavity is too large for guest molecules, whereas the cavity of CB6 is too small to encapsulate guest segments inside the CB cavity properly. It is possible to suppose that the size fit between CB and guest molecules might play a major role in binding affinity gain because this binding structure can directly affect internal interaction energy between CB and guest molecules and contribute to the amount of hydration penalty energy requirement when a complex is formed.

To explain this concretely, considering results from energy components can clarify these phenomena. Among the guest **2**, **3**, **4**, **5**, **6** and **8** complexes, CB–**2**, **3**, **4**, **5** and **6** complexes provide CB-size dependences in ΔE_{mm} and ΔG_{solv}. The value positively increases when increasing the CB size for the case of ΔE_{mm}, whereas ΔG_{solv} shows the opposite trend. On the other hand, guest **8** contributes the greatest value in the CB7 complex due to a larger substituent group with hydrophobicity, leading to a higher value in ΔE_{mm} due to internal interaction energy stabilization (Fig. 6b) and a larger value of ΔG_{solv} because of the high dehydration penalty requirement (Fig. 6c). We can confirm this using the solvation structures as depicted in Fig. 11. From the figure, only guest **8** can completely dehydrate water molecules from inside the CB7 cavity. By contrast, other guest molecules can totally displace the water in CB6 and partially dehydrate in the case of a bigger CB size. We have to note that guests **4** and **6** show relatively greater values of ΔE_{mm} (Fig. 6b) and ΔG_{solv} (Fig. 6c) due to positively charged molecules. However, compensation between the two terms can provide reasonable ΔG_{bind} values as shown in Fig. 6a.

4. Conclusions

In this study, we employed the 3D-RISM theory together with traditional MD simulations to investigate the binding affinity and solvation structure in host–guest systems, in which host and guest molecules are CBs with different sizes and amino acids. From our results, the binding features of CB–guest binding were first clarified. We found that the CB7–**1** and CB8–**1** complexes provide the exclusion binding complex, whereas the rest of the complexes give the inclusion binding complex. Moreover, the unbound states from CB7–**1** and CB8–**1** complexes, apart from forming typical binding complexes (exclusion or inclusion binding), were also observed. This unbound state was obtained in a small amino acid, guest **1** in this study. It may be noted that this state has possibly been found in the relatively small guest molecules having polar properties. Therefore, before investigating the small guest molecules on a CB–guest complex, all structures in a trajectory should be carefully checked.

From the binding affinity gains, we divided complexes into two groups: (I) the highest binding affinities were found in CB8 and (II) otherwise in CB7.

Glycine (**1**) and tryptophan (**7**) provide the greatest binding affinity for CB8 due to stabilization from HB and van der Waals interactions. However, CB–**7** complexes show higher values owing to the size fit between the CB cavity and guest **7**. In the case of the rest of the guest molecules, phenylalanine (**2**) and its derivatives provide the greatest binding affinity for CB7. The substitution of the *tert*-butyl ($-C(CH_3)_3$) group at the *para*-position in guest **2**, leading to guest **8**, shows an outstanding binding affinity gain. This is because full dehydration was achieved and van der Waals interactions work well, indicating the size fit between the substituent of guest **8** and the CB7 cavity.

Two host molecules, CB7 and CB8, were employed in this study. The

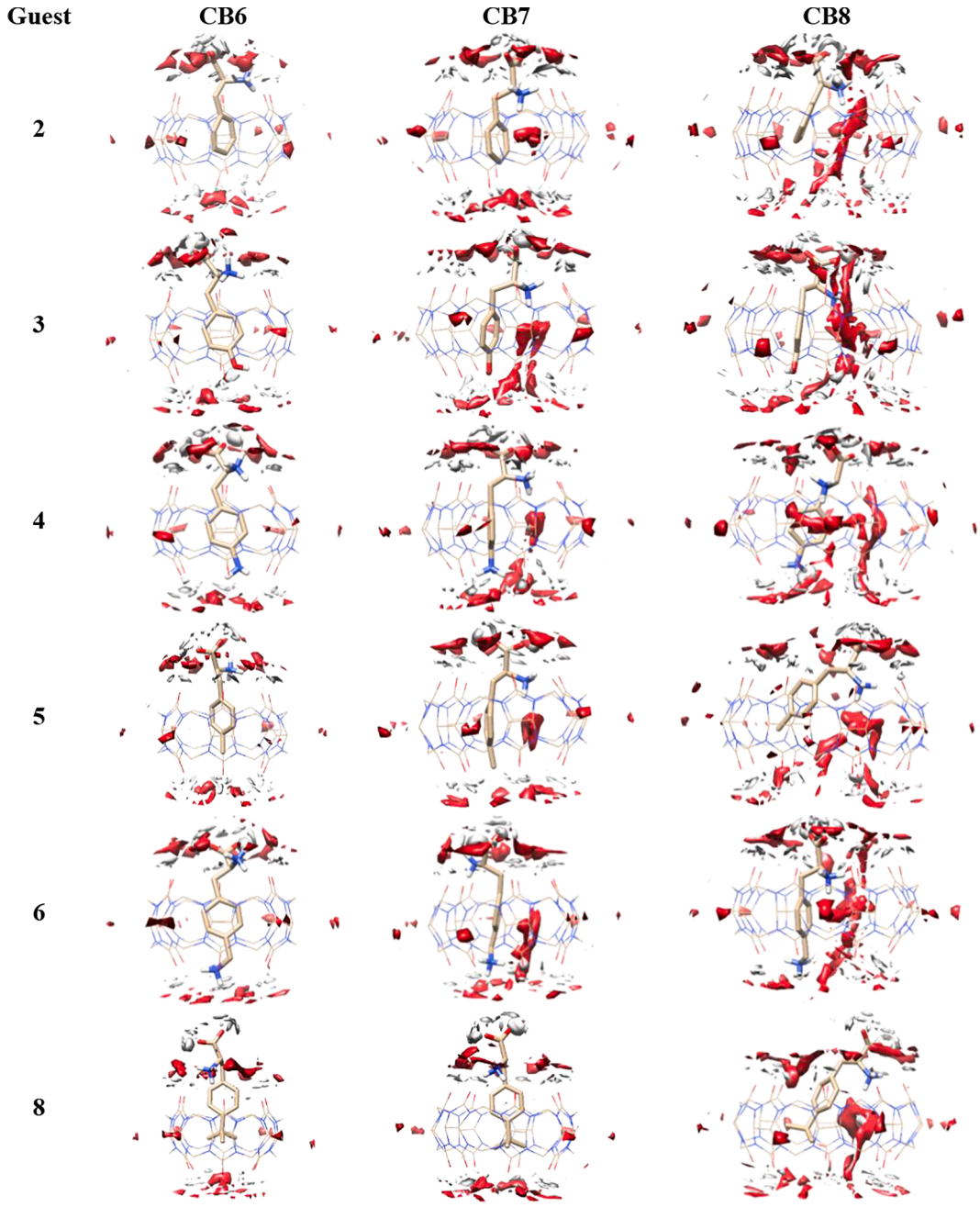

Fig. 11. Solvation structures of CB–guest complexes provide the greatest binding affinity gain in the CB7 complex, where guest = **2**, **3**, **4**, **5**, **6**, **7** and **8**. Isosurface plots of the 3D-DFs of the water oxygen and hydrogen with $g(\boldsymbol{r}) = 4.0$ are depicted in red and white, respectively.

only difference between these two host molecules is the number of members constituting the CB ring, and there does not seem to be any major structural difference. However, as our study revealed, such minor differences have a significant impact on the molecular recognition mechanism.

We have to note that the binding affinity can change when considering peptides or proteins because the sequence of amino acids also plays a crucial role in this system [16,17,19,32]. However, we believe that our findings can significantly contribute to the field of CB–guest binding by providing concrete information computationally, for example, how aromatic amino acids, like phenylalanine (guest **2**) and its derivatives, provide outstanding binding affinity gains with CB7 compared with the others. This useful knowledge can facilitate various applications such as sensors for specific amino acids, peptides and proteins of interest.

CRediT authorship contribution statement

Natthiti Chiangraeng: Conceptualization, Methodology, Formal analysis, Investigation, Visualization, Writing – original draft. **Haruyuki Nakano:** Writing – review & editing, Resources, Software. **Piyarat Nimmanpipug:** Conceptualization, Supervision, Writing – review & editing, Funding acquisition, Resources. **Norio Yoshida:** Conceptualization, Supervision, Writing – review & editing, Funding acquisition, Resources, Software.

Declaration of Competing Interest

The authors declare that they have no known competing financial interests or personal relationships that could have appeared to influence the work reported in this paper.

Data availability

Data will be made available on request.

Acknowledgments

Numerical calculations were partially conducted at the Research Center for Computational Science, Institute for Molecular Science, National Institutes of Natural Sciences (Project: 22-IMS-C076) and using MCRP-S at the Center for Computational Science, University of Tsukuba. Molecular graphics were produced using Chimera [64].

Funding sources

This research has received funding support from the NSRF via the Program Management Unit for Human Resources & Institutional Development, Research, and Innovation [grant number B13F660056]. Norio Yoshida is grateful for financial support from the Japan Society for the Promotion of Science (JSPS) KAKENHI (Grant Nos. 19H02677 and 22H05089). This work is also supported by the MEXT Program: Data Creation and Utilization-Type Material Research and Development Project (Grant No. JPMXP1122714694).

Appendix A. Supplementary data

Supplementary data to this article can be found online at https://doi.org/10.1016/j.molliq.2023.122503.

References

[1] A.R. Urbach, V. Ramalingam, Molecular recognition of amino acids, peptides, and proteins by cucurbit[*n*]uril receptors, Isr. J. Chem. 51 (2011) 664–678.
[2] S.J. Barrow, S. Kasera, M.J. Rowland, J. del Barrio, O.A. Scherman, Cucurbituril-Based Molecular Recognition, Chem. Rev. 115 (2015) 12320–12406.
[3] N. Yoshida, Role of Solvation in Drug Design as Revealed by the Statistical Mechanics Integral Equation Theory of Liquids, J. Chem. Inf. Model. 57 (2017) 2646–2656.
[4] E. Masson, X. Ling, R. Joseph, L. Kyeremeh-Mensah, X. Lu, Cucurbituril chemistry: A tale of supramolecular success, RSC Adv. 2 (2012) 1213–1247.
[5] D. Das, K.I. Assaf, W.M. Nau, Applications of Cucurbiturils in Medicinal Chemistry and Chemical Biology, Front. Chem. 7 (2019) 619.
[6] N. Chiangraeng, H. Nakano, P. Nimmanpipug, N. Yoshida, Theoretical Analysis of the Role of Water in Ligand Binding to Cucurbit[n]uril of Different Sizes, J. Phys. Chem. B. 127 (2023) 3651–3662.
[7] K. Bodoor, M.I. El-Barghouthi, D.F. Alhamed, K.I. Assaf, L. Alrawashdeh, Cucurbit[7]uril recognition of glucosamine anomers in water, J. Mol. Liq. 358 (2022), 119178.
[8] L.A. Logsdon, C.L. Schardon, V. Ramalingam, S.K. Kwee, A.R. Urbach, Nanomolar Binding of Peptides Containing Noncanonical Amino Acids by a Synthetic Receptor, J. Am. Chem. Soc. 133 (2011) 17087–17092.
[9] J.W. Lee, H.H.L. Lee, Y.H. Ko, K. Kim, H.I. Kim, Deciphering the specific high-affinity binding of cucurbit[7]uril to amino acids in water, J. Phys. Chem. B. 119 (2015) 4628–4636.
[10] L.M. Jones, E.H. Super, L.J. Batt, M. Gasbarri, F. Coppola, L.M. Bhebhe, B. T. Cheesman, A.M. Howe, P. Král, R. Coulston, S.T. Jones, Broad-spectrum extracellular antiviral properties of cucurbit[*n*]urils, ACS Infect. Dis. 8 (2022) 2084–2095.
[11] A. Buczkowski, Thermodynamic study of pH and sodium chloride impact on gemcitabine binding to cucurbit[7]uril in aqueous solutions, J. Mol. Liq. 345 (2022), 117857.
[12] A. Buczkowski, P. Tokarz, A. Stepniak, J. Lewkowski, A. Rodacka, B. Palecz, Spectroscopic and calorimetric studies of interactions between mitoxantrone and cucurbituril Q7 in aqueous solutions, J. Mol. Liq. 290 (2019), 111190.
[13] E. Delgado-Pinar, A.J.M. Valente, J. Sérgio Seixas de Melo, A comprehensive photophysical and NMR investigation on the interaction of a 4-methylumbelliferone derivative and cucurbit[7]uril, J. Mol. Liq. 277 (2019) 1026–1034.
[14] M.S. Mokhtar, A.A. Elbashir, F.E.O. Suliman, Spectroscopic and molecular simulation studies on the interaction of imazaquin herbicide with cucurbiturils (*n* = 6–8), J. Mol. Struct. 1274 (2023), 134444.
[15] A. Mehranfar, M. Izadyar, A.N. Shamkhali, A joint MD/QM study on the possibility of alkaloids detection by cucurbiturils and graphene oxide-cucurbituril composites, J. Mol. Liq. 272 (2018) 963–972.
[16] L.C. Smith, D.G. Leach, B.E. Blaylock, O.A. Ali, A.R. Urbach, Sequence-Specific, Nanomolar Peptide Binding via Cucurbit[8]uril-Induced Folding and Inclusion of Neighboring Side Chains, J. Am. Chem. Soc. 137 (2015) 3663–3669.
[17] M.E. Bush, N.D. Bouley, A.R. Urbach, Charge-mediated recognition of N-terminal tryptophan in aqueous solution by a synthetic host, J. Am. Chem. Soc. 127 (2005) 14511–14517.
[18] D.M. Bailey, A. Hennig, V.D. Uzunova, W.M. Nau, Supramolecular tandem enzyme assays for multiparameter sensor arrays and enantiomeric excess determination of amino acids, Chem. - A Eur. J. 14 (2008) 6069–6077.
[19] J.M. Chinai, A.B. Taylor, L.M. Ryno, N.D. Hargreaves, C.A. Morris, P.J. Hart, A. R. Urbach, Molecular recognition of insulin by a synthetic receptor, J. Am. Chem. Soc. 133 (2011) 8810–8813.
[20] F. Ma, X. Zheng, L. Xie, Z. Li, Sequence-dependent nanomolar binding of tripeptides containing N-terminal phenylalanine by Cucurbit[7]uril: A theoretical study, J. Mol. Liq. 328 (2021), 115479.
[21] P. Shan, R. Lin, M. Liu, Z. Tao, X. Xiao, J. Liu, Recognition of glycine by cucurbit[5]uril and cucurbit[6]uril: A comparative study of exo- and *endo*-binding, Chinese Chem. Lett. 32 (2021) 2301–2304.
[22] C. Jiang, Z. Song, M. Fizir, P. Yang, M. Liu, P. Dramou, H. He, Host–guest interaction between cucurbit[6]uril and chain amino acids, Chem. Phys. Lett. 783 (2021), 139039.
[23] F. Biedermann, W.M. Nau, H.-J. Schneider, The Hydrophobic Effect Revisited-Studies with Supramolecular Complexes Imply High-Energy Water as a Noncovalent Driving Force, Angew. Chemie Int. Ed. 53 (2014) 11158–11171.
[24] F. Biedermann, V.D. Uzunova, O.A. Scherman, W.M. Nau, A. De Simone, Release of high-energy water as an essential driving force for the high-affinity binding of cucurbit[*n*]urils, J. Am. Chem. Soc. 134 (2012) 15318–15323.
[25] F. Biedermann, M. Vendruscolo, O.A. Scherman, A. De Simone, W.M. Nau, Cucurbit[8]uril and blue-box: High-energy water release overwhelms electrostatic interactions, J. Am. Chem. Soc. 135 (2013) 14879–14888.
[26] N. Yoshida, T. Imai, S. Phongphanphanee, A. Kovalenko, F. Hirata, Molecular recognition in biomolecules studied by statistical-mechanical integral-equation theory of liquids, J. Phys. Chem. B. 113 (2009) 873–886.
[27] F. Hirata, Molecular Theory of Solvation, Kluwer, Dordrecht, The Netherlands, 2003.
[28] S.J. Singer, D. Chandler, Free energy functions in the extended RISM approximation, Mol. Phys. 55 (1985) 621–625.
[29] M. Sugita, I. Onishi, M. Irisa, N. Yoshida, F. Hirata, Molecular recognition and self-organization in life phenomena studied by a statistical mechanics of molecular liquids, the RISM/3D-RISM theory, Molecules. 26 (2021) 271.
[30] T. Imai, Molecular theory of partial molar volume and its applications to biomolecular systems, Condens. Matter Phys. 10 (2007) 343–361.
[31] P. Rajgariah, A.R. Urbach, Scope of amino acid recognition by cucurbit[8]uril, J. Incl. Phenom. Macrocycl. Chem. 62 (2008) 251–254.
[32] M.V. Rekharsky, H. Yamamura, Y.H. Ko, N. Selvapalam, K. Kim, Y. Inoue, Sequence recognition and self-sorting of a dipeptide by cucurbit[6]uril and cucurbit[7]uril, Chem. Commun. (2008) 2236–2238.
[33] R. Dennington, T.A. Keith, J.M. Millam, GaussView Version 6 (2019).
[34] Y. Kasai, N. Yoshida, H. Nakano, Theoretical analysis of salt effect on intramolecular proton transfer reaction of glycine in aqueous NaCl solution, J. Mol. Liq. 200 (2014) 32–37.
[35] Y. Kasai, N. Yoshida, H. Nakano, Theoretical analysis of co-solvent effect on the proton transfer reaction of glycine in a water-acetonitrile mixture, J. Chem. Phys. 142 (2015), 204103.
[36] H.J. Buschmann, E. Schollmeyer, L. Mutihac, The formation of amino acid and dipeptide complexes with α-cyclodextrin and cucurbit[6]uril in aqueous solutions studied by titration calorimetry, Thermochim. Acta. 399 (2003) 203–208.
[37] M.J. Frisch, G.W. Trucks, H.B. Schlegel, G.E. Scuseria, M.A. Robb, J.R. Cheeseman, G. Scalmani, V. Barone, G.A. Petersson, H. Nakatsuji, X. Li, M. Caricato, A. V Marenich, J. Bloino, B.G. Janesko, R. Gomperts, B. Mennucci, H.P. Hratchian, J. V Ortiz, A.F. Izmaylov, J.L. Sonnenberg, D. Williams-Young, F. Ding, F. Lipparini, F. Egidi, J. Goings, B. Peng, A. Petrone, T. Henderson, D. Ranasinghe, V.G. Zakrzewski, J. Gao, N. Rega, G. Zheng, W. Liang, M. Hada, M. Ehara, K. Toyota, R. Fukuda, J. Hasegawa, M. Ishida, T. Nakajima, Y. Honda, O. Kitao, H. Nakai, T. Vreven, K. Throssell, J.A. Montgomery, Jr., J.E. Peralta, F. Ogliaro, M.J. Bearpark, J.J. Heyd, E.N. Brothers, K.N. Kudin, V.N. Staroverov, T.A. Keith, R. Kobayashi, J. Normand, K. Raghavachari, A.P. Rendell, J.C. Burant, S.S. Iyengar, J. Tomasi, M. Cossi, J.M. Millam, M. Klene, C. Adamo, R. Cammi, J.W. Ochterski, R.L. Martin, K. Morokuma, O. Farkas, J.B. Foresman, D.J. Fox, Gaussian 16, Rev. C.01, Gaussian, Inc., Wallingford CT, 2019.
[38] V. Barone, M. Cossi, Conductor Solvent Model, J. Phys. Chem. A. 102 (1998) 1995–2001.
[39] M. Cossi, N. Rega, G. Scalmani, V. Barone, Energies, structures, and electronic properties of molecules in solution with the C-PCM solvation model, J. Comput. Chem. 24 (2003) 669–681.
[40] J. Wang, W. Wang, P.A. Kollman, D.A. Case, Automatic atom type and bond type perception in molecular mechanical calculations, J. Mol. Graph. Model. 25 (2006) 247–260.
[41] J. Wang, P. Cieplak, P.A. Kollman, How Well Does a Restrained Electrostatic Potential (RESP) Model Perform in Calculating Conformational Energies of Organic and Biological Molecules? J. Comput. Chem. 21 (2000) 1049–1074.
[42] D.A. Case, K. Belfon, I.Y. Ben-Shalom, S.R. Brozell, D.S. Cerutti, T.E. Cheatham III, V.W.D. Cruzeiro, T.A. Darden, R.E. Duke, G. Giambasu, M.K. Gilson, H. Gohlke, A. W. Goetz, R. Harris, S. Izadi, S.A. Izmailov, K. Kasavajhala, A. Kovalenko, R. Krasny, T. Kurtzman, T.S. Lee, S. LeGrand, P. Li, C. Lin, J. Liu, T. Luchko, R. Luo, V. Man, K.M. Merz, Y. Miao, O. Mikhailovskii, G. Monard, H. Nguyen, A. Onufriev, F. Pan, S. Pantano, R. Qi, D.R. Roe, A. Roitberg, C. Sagui, S. Schott-Verdugo, J. Shen, C.L. Simmerling, N.R. Skrynnikov, J. Smith, J. Swails, R.C. Walker,

J. Wang, L. Wilson, R.M. Wolf, X. Wu, Y. Xiong, Y. Xue, Amber 20, University of California, San Francisco, 2020.
[43] H.J.C. Berendsen, J.P.M. Postma, W.F. van Gunsteren, A. DiNola, J.R. Haak, Molecular dynamics with coupling to an external bath, J. Chem. Phys. 81 (1984) 3684–3690.
[44] H.C. Andersen, Rattle: A "velocity" version of the shake algorithm for molecular dynamics calculations, J. Comput. Phys. 52 (1983) 24–34.
[45] D.R. Roe, T.E. Cheatham, PTRAJ and CPPTRAJ: Software for processing and analysis of molecular dynamics trajectory data, J. Chem. Theory Comput. 9 (2013) 3084–3095.
[46] A. Kovalenko, F. Hirata, Potentials of mean force of simple ions in ambient aqueous solution. II. Solvation structure from the three-dimensional reference interaction site model approach, and comparison with simulations, J. Chem. Phys. 112 (2000) 10403–10417.
[47] A. Kovalenko, F. Hirata, Potential of mean force between two molecular ions in a polar molecular solvent: A study by the three-dimensional reference interaction site model, J. Phys. Chem. B. 103 (1999) 7942–7957.
[48] Y. Maruyama, F. Hirata, Modified Anderson Method for Accelerating 3D-RISM Calculations Using Graphics Processing Unit, J. Chem. Theory Comput. 8 (2012) 3015–3021.
[49] Y. Maruyama, N. Yoshida, H. Tadano, D. Takahashi, M. Sato, F. Hirata, Massively parallel implementation of 3D-RISM calculation with volumetric 3D-FFT, J. Comput. Chem. 35 (2014) 1347–1355.
[50] N. Yoshida, The Reference Interaction Site Model Integrated Calculator (RISMiCal) program package for nano- and biomaterials design, IOP Conf. Ser. Mater. Sci. Eng. 773 (2020), 012062.
[51] L.M. Grimm, S. Spicher, B. Tkachenko, P.R. Schreiner, S. Grimme, F. Biedermann, The Role of Packing, Dispersion, Electrostatics, and Solvation in High-Affinity Complexes of Cucurbit[n]urils with Uncharged Polar Guests, Chem. – A Eur. J. 28 (2022) e202200529.
[52] K.I. Assaf, M. Florea, J. Antony, N.M. Henriksen, J. Yin, A. Hansen, Z.W. Qu, R. Sure, D. Klapstein, M.K. Gilson, S. Grimme, W.M. Nau, HYDROPHOBE Challenge: A Joint Experimental and Computational Study on the Host-Guest Binding of Hydrocarbons to Cucurbiturils, Allowing Explicit Evaluation of Guest Hydration Free-Energy Contributions, J. Phys. Chem. B. 121 (2017) 11144–11162.
[53] N.S. Venkataramanan, A. Suvitha, Y. Kawazoe, Unravelling the nature of binding of cubane and substituted cubanes within cucurbiturils: A DFT and NCI study, J. Mol. Liq. 260 (2018) 18–29.
[54] O. Danylyuk, Exploring cucurbit[6]uril-peptide interactions in the solid state: Crystal structure of cucurbit[6]uril complexes with glycyl-containing dipeptides, CrystEngComm. 19 (2017) 3892–3897.
[55] T. Imai, A. Kovalenko, F. Hirata, Partial molar volume of proteins studied by the three-dimensional reference interaction site model theory, J. Phys. Chem. B. 109 (2005) 6658–6665.
[56] N. Yoshida, S. Phongphanphanee, F. Hirata, Selective Ion Binding by Protein Probed with the Statistical Mechanical Integral Equation Theory, J. Phys. Chem. B. 111 (2007) 4588–4595.
[57] T. Imai, A. Kovalenko, F. Hirata, Solvation thermodynamics of protein studied by the 3D-RISM theory, Chem. Phys. Lett. 395 (2004) 1–6.
[58] T. Imai, Y. Harano, M. Kinoshita, A. Kovalenko, F. Hirata, A theoretical analysis on hydration thermodynamics of proteins, J. Chem. Phys. 125 (2006), 024911.
[59] S. Tanimoto, N. Yoshida, T. Yamaguchi, S.L. Ten-No, H. Nakano, Effect of Molecular Orientational Correlations on Solvation Free Energy Computed by Reference Interaction Site Model Theory, J. Chem. Inf. Model. 59 (2019) 3770–3781.
[60] V. Sergiievskyi, G. Jeanmairet, M. Levesque, D. Borgis, Solvation free-energy pressure corrections in the three dimensional reference interaction site model, J. Chem. Phys. 143 (2015), 184116.
[61] C. Márquez, R.R. Hudgins, W.M. Nau, Mechanism of Host-Guest Complexation by Cucurbituril, J. Am. Chem. Soc. 126 (2004) 5806–5816.
[62] F. Biedermann, H.-J. Schneider, Experimental Binding Energies in Supramolecular Complexes, Chem. Rev. 116 (2016) 5216–5300.
[63] Y. Harano, M. Kinoshita, Large gain in translational entropy of water is a major driving force in protein folding, Chem. Phys. Lett. 399 (2004) 342–348.
[64] E.F. Pettersen, T.D. Goddard, C.C. Huang, G.S. Couch, D.M. Greenblatt, E.C. Meng, T.E. Ferrin, UCSF Chimera - a visualization system for exploratory research and analysis, J. Comput. Chem. 25 (2004) 1605–1612.